Pure Appl. Chem., Vol. 80, No. 11, pp. 2537–2542, 2008.
doi:10.1351/pac200880112537

Novel-shaped $LiNi_{1/3}Co_{1/3}Mn_{1/3}O_2$ prepared by a hydroxide coprecipitation method*

Zexun Tang[1,2], Deshu Gao[1,‡], Ping Chen[1,2], Zhaohui Li[1], and Qiang Wu[2]

[1]Key Laboratory of Environmentally Friendly Chemistry and Applications of Ministry of Education, College of Chemistry, Xiangtan University, Xiangtan, Hunan 411105, China; [2]L & F Material Co. Ltd., Daegu, 704-220, South Korea

Abstract: $Ni_{1/3}Co_{1/3}Mn_{1/3}(OH)_2$, a precursor of $LiNi_{1/3}Co_{1/3}Mn_{1/3}O_2$ in new-generation Li-ion batteries, was prepared by a hydroxide coprecipitation method. Scanning electronic microscopy (SEM) micrographs reveal that the precursor particles thus obtained, show regular shape with uniform size under optimized conditions. X-ray diffraction (XRD) indicates that well-ordered layer-structured $LiNi_{1/3}Co_{1/3}Mn_{1/3}O_2$ was prepared after calcination at high temperature. The final product exhibited a spherical morphology with uniform size distribution (10 μm in diameter). At the terminal charging voltage of 4.3 and 4.5 V (vs. Li/Li^+), the testing cells of $LiNi_{1/3}Co_{1/3}Mn_{1/3}O_2$ delivered a specific capacity of 161.2 and 184.1 $mAh{\cdot}g^{-1}$, respectively. The high capacity retention of 98.0 and 96.1 % after charging to 4.3 and 4.5 V for 50 cycles, respectively, indicates that this material displays excellent cycling stability even at high cut-off voltage.

Keywords: hydroxide coprecipitation; lithium-ion batteries; precursor; electrochemical performance.

INTRODUCTION

Nowadays, Li-ion batteries have gained huge momentum in the face of the increasing energy source demand for portable electronic products. For improving the performance of Li-batteries, it is very important to find suitable cathode materials. $LiCoO_2$ has been the most prevalent commercial cathode material for years [1,2]. However, some inherent drawbacks, such as the relatively high cost of cobalt, lack of safety, and environmental toxicity, have provided incentives to seek suitable substitutes. Recently, $LiNi_{1/3}Co_{1/3}Mn_{1/3}O_2$ has attracted intensive attention owing to its high specific capacity, long cyclic life, and excellent safety properties [3,4]. At the same time, it is cheaper than $LiCoO_2$.

$LiNi_{1/3}Co_{1/3}Mn_{1/3}O_2$ has layered hexagonal structure, it can be regarded as a solid solution of $LiCoO_2$ and $LiNi_{0.5}Mn_{0.5}O_2$. In this solid solution, the valence states of Ni, Co, and Mn are +2, +3, and +4, respectively [5]. During charge–discharge process, only divalent Ni and trivalent Co are electroactive through $Ni^{2+/4+}$ and $Co^{3+/4+}$ redox couples and tetravalent Mn ion is inactive. However, the electrochemically inactive Mn plays an essential role of supporting the host structure during Li^+ de-/intercalation and contributes stable cycling performance [4,6]. As a complex composite, however, it is difficult to synthesize phase-pure $LiNi_{1/3}Co_{1/3}Mn_{1/3}O_2$ by a simple mixed calcination method [7].

---

*Paper based on a presentation at the 3rd International Symposium on Novel Materials and Their Synthesis (NMS-III) and the 17th International Symposium on Fine Chemistry and Functional Polymers (FCFP-XVII), 17–21 October 2007, Shanghai, China. Other presentations are published in this issue, pp. 2231–2563.
‡Corresponding author: E-mail: gaod@xtu.edu.cn

Because mechanical blending is incapable of achieving an intimate mix of the three kinds of transition metals, the resultant product is often inhomogeneous or impure, and delivers inferior electrochemical performance. It has been reported that a homogeneous precursor with good morphology can be produced by a coprecipitation method, whereby all the components are mixed at an atomic level [8,9]. Calcination of the resultant precursor with Li salt gives rise to well-ordered layer-structured $LiNi_{1/3}Co_{1/3}Mn_{1/3}O_2$ powders. These samples often show high energy density and superior cycle performance. Lee et al. have done much work on optimizing reaction parameters during the hydroxide coprecipitation process, such as pH value, stirring speed, and concentrations of NH_4OH, and have achieved some remarkable results [8]. However, there are few reports in which the morphology and electrochemical performance under various molar ratios of chelating agent to transition-metal ions have been investigated. In this paper, we report the preparation of hydroxide precursor powders using various amounts of ammonia, and discuss the relationship between morphology and electrochemical characteristics.

EXPERIMENTAL

$Ni_{1/3}Co_{1/3}Mn_{1/3}(OH)_2$ was prepared by well-controlled deposition. A solution of $NiSO_4$, $CoSO_4$, and $MnSO_4$ (Ni:Co:Mn = 1:1:1, molar ratio) was fed into a continuously stirred reactor, at the same time, the solution of NH_4OH and NaOH were also dripped into the reactor, respectively. The resultant sediment was filtered, washed, and dried. The mixture of this dried precursor and Li salt was sintered at 850 °C for 10 h to give $LiNi_{1/3}Co_{1/3}Mn_{1/3}O_2$.

Scanning electron microscopy (SEM Philip XL30) was used to observe the morphology of the particles. X-ray diffraction (XRD, Bruker D8) was used to characterize the crystal structure of the final product.

Charge–discharge tests were performed on a LAND CT2001A battery test system with model cell at 25 °C. The cell consisted of a positive $LiNi_{1/3}Co_{1/3}Mn_{1/3}O_2$ electrode and a negative Li metal electrode, using a porous polypropylene membrane as the separator. The electrolyte was 1 M $LiPF_6$ in the mixed solvent comprising dimethyl carbonate (DMC)/ethyl methyl carbonate (EMC)/ethylene carbonate (EC) (1:1:1, w/w).

RESULTS AND DISCUSSION

Morphology of precursor and $LiNi_{1/3}Co_{1/3}Mn_{1/3}O_2$

For preparing homogeneous precursor, $Ni_{1/3}Co_{1/3}Mn_{1/3}(OH)_2$, it is important to employ chelating agent for assisting deposition and controlling reaction conditions [8,9]. As a popular chelating agent, ammonia plays a significant role for improving uniformity and suppressing phase separation. Moreover, it often makes the products have regular morphology like sphere and high tap-density. When the depositing conditions were well controlled, the morphology of the precursors could be controlled as desired.

In this work, we investigated the influence of ammonia amount on the morphology of precursors. During depositing process, the pH value of the suspend solution was controlled at 11.5 by NaOH solution, and the reaction temperature, stirring speed, and feeding rate of the solution of sulfates were maintained at 70 °C, 800 rpm, and 20 $mL \cdot min^{-1}$, respectively. Four kinds of samples with various morphologies (denoted as A, B, C, and D) were prepared under various molar ratios of ammonia to metal ions (0.5:1, 1:1, 1.5:1, and 2:1), as shown in Fig. 1.

During the precipitation process, chelating agents reacted with metal ions leading to some crystal nuclei at first [9]. These crystal nuclei grew up to form the visible spherical particles (marked by arrow in Figs. 1A and 1B), which were usually called as primary particles. The primary particles piled together to form secondary particles with large size. It can be observed, from Fig. 1, that the amount of

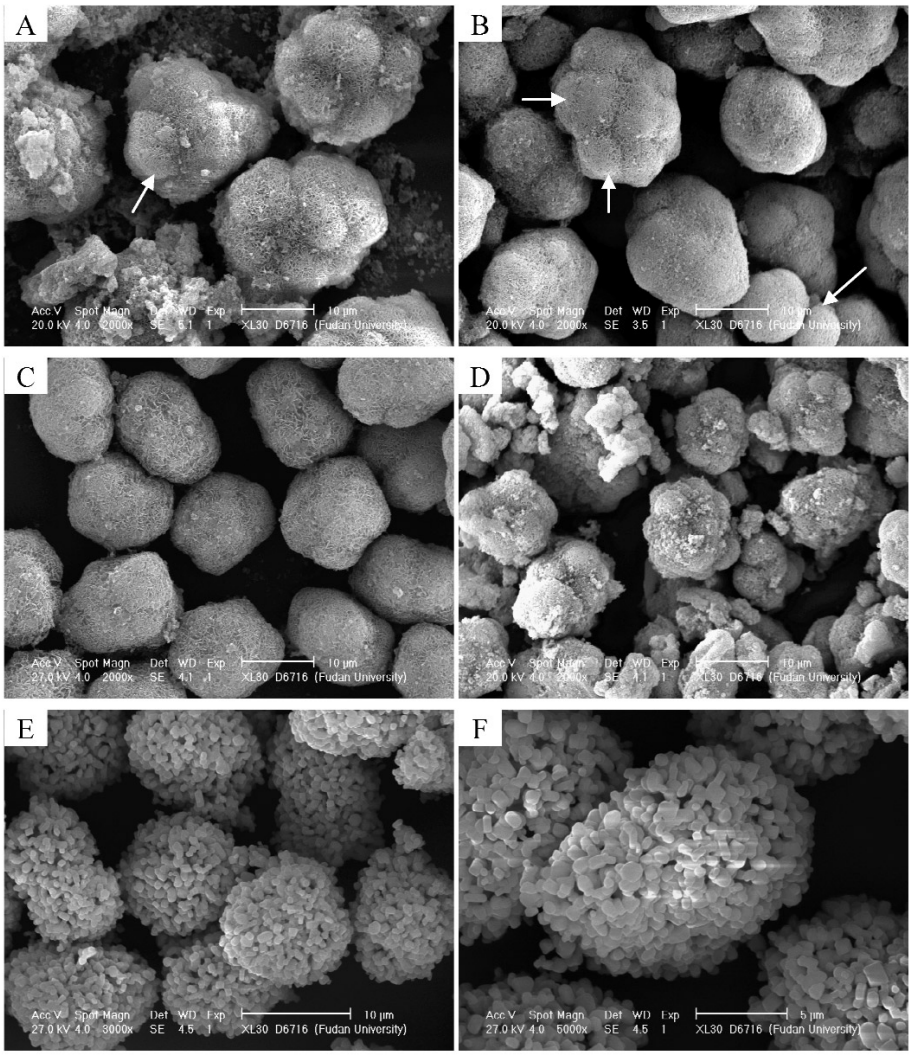

Fig. 1 SEM images of precursor and $LiNi_{1/3}Co_{1/3}Mn_{1/3}O_2$ powders. Images A, B, C and D were precursor powders synthesized at different molar ratios of ammonia to metal ions: 0.5:1 (A), 1:1 (B), 1.5:1 (C), and 2.0:1 (D). Images E and F were $LiNi_{1/3}Co_{1/3}Mn_{1/3}O_2$ powders prepared by calcined precursor C with Li_2CO_3 at 850 °C for 10 h: (E) low and (F) high magnification.

ammonia dramatically affected the morphology of precursors. The secondary particles became more and more regular and uniform with the molar ratio of ammonia to metal ions increasing from 0.5:1 to 1.5:1. Precursor A was composed of some irregular secondary particles, which was piled by some smaller spherical particles (primary one). With the increasing amount of ammonia, the primary particles piled much more tightly and thus the secondary particles turned to be regularly quasi-spherical shape. At the same time, the size distribution of the secondary particles became narrow (precursors B and C). Precursor C is the most uniform and well-separated particles with smooth surface. When the molar ratio of ammonia to metal ions adds up to 2:1, the high amount of ammonia deteriorated the superior morphology, resulting in a broad size distribution and irregular shape (precursor D). It suggests that there are not enough nuclei for metal ions to grow up during deposition process at low ammonia amount. The excessive metal ions react immediately with OH^- anions without being chelated at prior

so there often comes out some agglomerated pieces (Fig. 1A). However, at high amount of ammonia, excessive crystal nuclei formed leading to yield loose piled secondary particles and many relatively smaller particles (Fig. 1D).

Sintering precursor C with Li_2CO_3 powders, $LiNi_{1/3}Co_{1/3}Mn_{1/3}O_2$ was produced with a spherical morphology as shown in Figs. 1E and 1F. It is clear that the microstructure of the secondary particles changed much after high-temperature calcination. Uniform grain-like primary particles (about 500 nm in diameter) piled together to form spherical or quasi-spherical secondary particles (about 10 μm in diameter). The diameter of secondary particles was about 5 μm smaller than that of the precursor powders. This kind of particle has an attractive tap-density of 2.15 $g \cdot cm^{-3}$.

XRD pattern of $LiNi_{1/3}Co_{1/3}Mn_{1/3}O_2$

Figure 2 shows a typical XRD pattern of $LiNi_{1/3}Co_{1/3}Mn_{1/3}O_2$ without any impurity phase. The XRD pattern can be indexed on the basis of the α-$NaFeO_2$ structure (space group: Rm). The calculated lattice parameters (a = 2.8577 Å, c = 14.2277 Å) are close to those of the reported values [3,10]. In the XRD pattern, the integrated peak splits of (006)/(102) and (108)/(110) are known to be an indicator of characteristics of the layered structure like $LiCoO_2$ and $LiNiO_2$ [11–13]. The clear splits (006)/(102) and (108)/(110) in Fig. 2 reveal the layered structure formed. Generally, the integrated intensity ratio of (003) to (104) (I_{003}/I_{104}) can be used to characterize the degree of the cation mixing. It could be neglected when this value is larger than 1.2 [14]. The ratio of I_{003}/I_{104} is 1.43 for the obtained products in this paper, indicating no undesirable cation mixing. All these proofs confirm that the well-ordered layer-structured $LiNi_{1/3}Co_{1/3}Mn_{1/3}O_2$ with high integrity was successfully prepared.

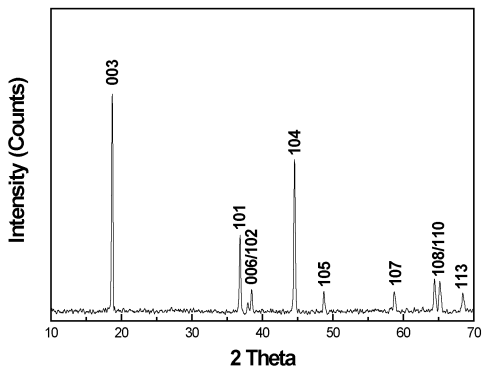

Fig. 2 Powder XRD pattern of $LiNi_{1/3}Co_{1/3}Mn_{1/3}O_2$.

Electrochemical property

Figure 3 shows the initial charge and discharge curves by cell voltage plotted vs. specific gravimetric capacity. The testing cells were charged and discharged at a constant current density of 0.1 C. The sample delivered a specific capacity of 161.2 and 184.1 $mAh \cdot g^{-1}$ after being charged to 4.3 and 4.5 V, respectively. It also exhibited a small irreversible capacity loss during the whole voltage range in Fig. 3, indicating that there was no conspicuous structure change during the first cycle.

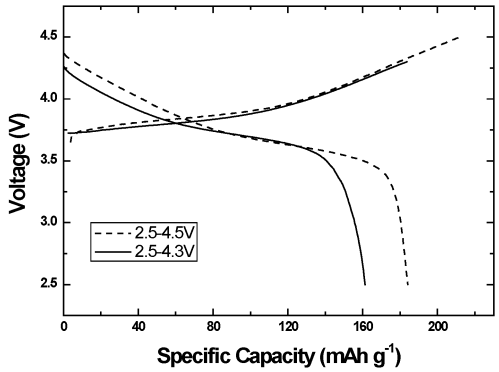

Fig. 3 Initial charge–discharge curves for $LiNi_{1/3}Co_{1/3}Mn_{1/3}O_2$ at different cut-off voltages of 2.5–4.3 and 2.5–4.5 V.

Figure 4 displays the cyclic performance of the first 50 cycles. After 50 cycles, the cells retained 98.0 and 96.1 % of the initial discharge capacity when charged to 4.3 and 4.5 V, respectively. Therefore, $LiNi_{1/3}Co_{1/3}Mn_{1/3}O_2$ presented excellent cyclic stability even at higher voltage, suggesting that the crystal structure should be stable and the side-reaction between cathode and electrolyte be greatly suppressed during charge and discharge.

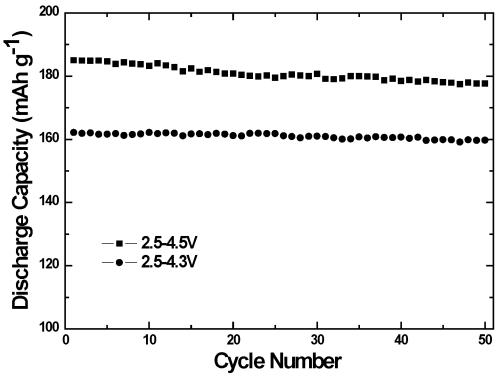

Fig. 4 Cycle performance of $LiNi_{1/3}Co_{1/3}Mn_{1/3}O_2$ cells at 0.1 C cycled to different upper cut-off voltages.

It is well known that the electrochemical property basically depended on the crystal structure and particle morphology [6,8]. Well-ordered layer structure can keep high integrity during charge and discharge. Moreover, uniform and regular particles of $LiNi_{1/3}Co_{1/3}Mn_{1/3}O_2$ powders may benefit to maintain the morphology and avoid agglomeration. The primary particles aggregate inter-connectedly forming some interspaces (Figs. 1E and 1F). Such a loose structure would well accommodate any volume changes of crystals with structural transition. On the other hand, the little vacancy usually benefits to the quicker migration of Li ions than the agglomerated materials during charge and discharge [6,15,16]. As a result, the cyclic performance of the obtained $LiNi_{1/3}Co_{1/3}Mn_{1/3}O_2$ enhances.

CONCLUSION

To optimize synthesis conditions, $LiNi_{1/3}Co_{1/3}Mn_{1/3}O_2$ powders with good morphology and superior electrochemical performance were obtained by hydroxide coprecipitation method. It was found that the

particles' morphology was dramatically affected by the reaction condition. Uniform and regular precursor particles could be produced when the molar ratio of ammonia to metal ions was 1.5:1. After calcination at 850 °C for 10 h, $LiNi_{1/3}Co_{1/3}Mn_{1/3}O_2$ with spherical shape and uniform particle size was prepared. XRD investigation revealed that the final product had a typical layered structure. It can deliver an initial discharge capacity of 161.2 and 184.1 $mAh \cdot g^{-1}$ when charged to 4.3 and 4.5 V (vs. Li/Li^+), respectively. After 50 cycles, the $LiNi_{1/3}Co_{1/3}Mn_{1/3}O_2$ materials show no obvious capacity fading even charged at a high voltage of 4.5 V.

REFERENCES

1. K. Mizushima, P. C. Jones, P. J. Wiseman, J. B. Goodenough. *Mater. Res. Bull.* **15**, 783 (1980).
2. J.-M. Tarascon, M. Armand. *Nature* **414**, 359 (2001).
3. T. Ohzuku, Y. Makimura. *Chem. Lett*. **7**, 642 (2001).
4. K. M. Shaju, G. V. Subba Rao, B. V. R. Chowdari. *Electrochim. Acta* **48**, 145 (2002).
5. W.-S. Yoon, C. P. Grey, M. Balasubramanian, X.-Q. Yang, D. A. Fisher, J. McBreen. *Electrochem. Solid-State Lett.* **7**, 53 (2004).
6. S.-H. Park, H.-S. Shin, S.-T. Myung, C. S. Yoon, K. Amine, Y.-K Sun. *Chem. Mater*. **17**, 6 (2005).
7. Y. J. Shin, W. J. Choi, Y. S. Hong, S. Yoon, K. S. Ryu, S. H. Chang. *Solid State Ionics* **177**, 515 (2006).
8. M.-H. Lee, Y.-J. Kang, S.-T. Myung, Y.-K. Sun. *Electrochim. Acta* **50**, 939 (2004).
9. P. He, H. R. Wang, L. Qi, T. Osaka. *J. Power Sources* **160**, 627 (2006).
10. T. H. Cho, S. M. Park, M. Yoshio. *Chem. Lett*. **6**, 704 (2004).
11. J. R. Dahn, U. Von sacken, A. V. Chadwick. *Solid State Ionics* **44**, 87 (1990).
12. Y. Gao, M. V. Yakovleva, W. B. Ebner. *Electrochem. Solid-State Lett*. **1**, 117 (1998).
13. Y. J. Huang, D. S. Gao, G. T. Lei, Z. H. Li, G. Y. Su. *Mater. Chem. Phys.* **106**, 354 (2007).
14. Z. L. Liu, A. S. Yu, J. Y. Lee. *J. Power Sources* **81**, 416 (1999).
15. Y. Fujii, H. Miura, N. Suzuki, T. Shoji, N. Nakayama. *J. Power Sources* **171**, 894 (2007).
16. K. M. Shaju, P. G. Bruce. *Adv. Mater*. **18**, 2330 (2006).